PAPER

Check for updates

Design, synthesis and cytotoxic activity of molecular hybrids based on quinolin-8-yloxy and cinnamide hybrids and their apoptosis inducing property†

Dalal Nasser Binjawhar, [ID] [a] Fawziah A. Al-Salmi,[b] Ola A. Abu Ali, [ID] [c] Maha Ali Alghamdi,[d] Eman Fayad, [ID] [d] Rasha Mohammed Saleem,[e] Islam Zaki [ID] *[f] and N. A. Farouk[g]

The present work aims at design and synthesis of a congeneric series of small hybrids 5 and 6a–i featuring the privileged quinoline scaffold tethered with 2-(arylamido)cinnamide moiety as potential anticancer tubulin polymerization inhibitors. Most of the synthesized hybrids 5 and 6a–i significantly inhibited the growth of the HepG2 cell line, with IC_{50} ranged from 2.46 to 41.31 μM. In particular, 2-(3,4,5-trimethoxybenzamido)-4-methoxycinnamide-quinoline hybrid 6e displayed potent IC_{50} value toward the examined cell line, and hence chosen for further mechanistic investigations. It is noteworthy that the antiproliferative action of compound 6e highly correlated well with its ability to inhibit tubulin polymerization. In addition, the most potent hybrid 6e demonstrated a significant modification in the cellular cycle distribution, in addition to provoke of apoptotic death within the tested HepG2 cell line. Furthermore, the mechanistic approach was confirmed by a substantial upregulation in the quantity of active caspase 9 by 5.81-fold relative to untreated control cells.

1. Introduction

Cancer is a major global health issue defined by accelerated and uncontrolled cellular proliferation of normal cells.[1] In addition, cancer is still ranked as one of the leading causes of death worldwide.[2] The marketed anticancer chemotherapeutic agents were accompanied with considerable negative impacts due to the dosage and duration of the treatment as well as the resistance developed against them.[3] As consequently, the search for new and less unsafe therapeutics with enhanced selectivity toward cancer cells remain a promising research field.[4] As a result, the most recent strategies aimed to discover and seek out certain biological markers crucial for cancerous cells such as aberrant, modified or overstated proteins.[5] In recent times, tubulin polymerization has been recognized as a significant molecular target for the search and development of anticancer drugs.[6] The polymerization of tubulin is necessary to form microtubules that have a crucial role in cellular functions, including the maintenance of cellular structure, intracellular transportation as well as mitotic spindle formation for cell division.[7,8] In recent decades, a wide range of natural compounds and synthetic components have been identified as anticancer drugs that interfere with tubulin-microtubule dynamics.[9–11] The clinical success of such agents demonstrates that enormous potential of this target to the design and development of new anti-tubulin polymerization compounds as effective targeted anticancer regimens.[12]

Quinoline scaffold (1-aza-naphthalene or benzo[b]pyridine) as an important class of N-biologically active heterocycles, represent a leading and promising heterocyclic pharmacophore.[13] The quinoline scaffold is a well-recognized for diverse pharmacological applications, various natural products and bioactive drug compounds incorporate quinoline framework.[14,15] Notable medicinal applications associated with the quinoline heterocycle includes anticancer, antiviral, antitubercular and many other biological properties with significant interest in the creation of beneficial quinoline-based anticancer compounds such as Campothecin, Topotecan and Irinotecan.[16–20]

[a]Department of Chemistry, College of Science, Princess Nourah bint Abdulrahman University, P.O. Box 84428, Riyadh 11671, Saudi Arabia

[b]Biology Department, College of Sciences, Taif University, P.O. Box 11099, Taif 21944, Saudi Arabia

[c]Department of Chemistry, College of Science, Taif University, P.O. Box 11099, Taif 21944, Saudi Arabia

[d]Department of Biotechnology, College of Sciences, Taif University, P.O. Box 11099, Taif 21944, Saudi Arabia

[e]Department of Laboratory Medicine, Faculty of Applied Medical Sciences, Al-Baha University, Al-Baha 65431, Saudi Arabia

[f]Pharmaceutical Organic Chemistry Department, Faculty of Pharmacy, Port Said University, Port Said 42526, Egypt. E-mail: Eslam.Zaki@pharm.psu.edu.eg

[g]Department of Chemistry, Faculty of Science, Port Said University, Port Said 42526, Egypt

In parallel, cinnamide pharmacophore is regarded an interesting scaffold in the realm of medicinal and pharmaceutical chemistry.[21] Cinnamide-based compounds also displayed a wide plethora of biological properties including anticancer activities via different mechanism of action such as the inhibition of tyrosine kinase, cell cycle arrest and so on.[22–26] Moreover, cinnamide moiety is commonly exploited as a potential pharmacologically active component in the construction of tubulin assembly inhibitors.[27]

Molecular hybridization strategy of a well-known pharmacophores could provide effective in exerting a beneficial role for drug-sensitive cancer and also for drug-resistance cancer.[28,29] Incorporation of heterocyclic moiety such as the quinoline moiety into anticancer agents was succeeded as a new strategy to produce hybrid molecules with potent anticancer activity.[30] In this regard, we perform the current study to optimize the cytotoxic potential after incorporation of quinoline moiety with cinnamide scaffold and investigate their ability to interfere with tubulin polymerization as well as apoptosis induction.[31,32] In addition, the structure activity relationship (SAR) of the target hybrids was achieved through changes in 2-(arylamido)

substituents (R^1) with either (3,4,5-trimethoxybenzamido) or (3,4-dimethoxybenzamido) groups as well as variation of the type of substituents (R^2) on the cinnamide moiety to include electron-donating and electron-withdrawing groups (Fig. 1). All the herein reported quinoline-cinnamide hybrids 5 and 6a–i were screened for their cytotoxic action against liver HepG2 cancerous cell line. The most promising member in the cytotoxicity assay was subsequently investigated for its activity against tubulin inhibitory activity, as well as its effect on cellular cycle distribution and ability to induce apoptosis.

2. Results and discussion

2.1. Chemistry

The strategy to synthesize the target quinoline-cinnamide hybrids 5 and 6a–i is depicted in Scheme 1. Initiated from 8-hydroxyquinoline 1, it was reacted with 2-chloroacetic acid in the presence of K_2CO_3 using dimethylformamide as solvent. The reaction was carried out at reflux temperature to afford 2-(quinoline-8-yloxy)acetic acid 2 that was subjected to esterification reaction in the presence of pure ethanol and
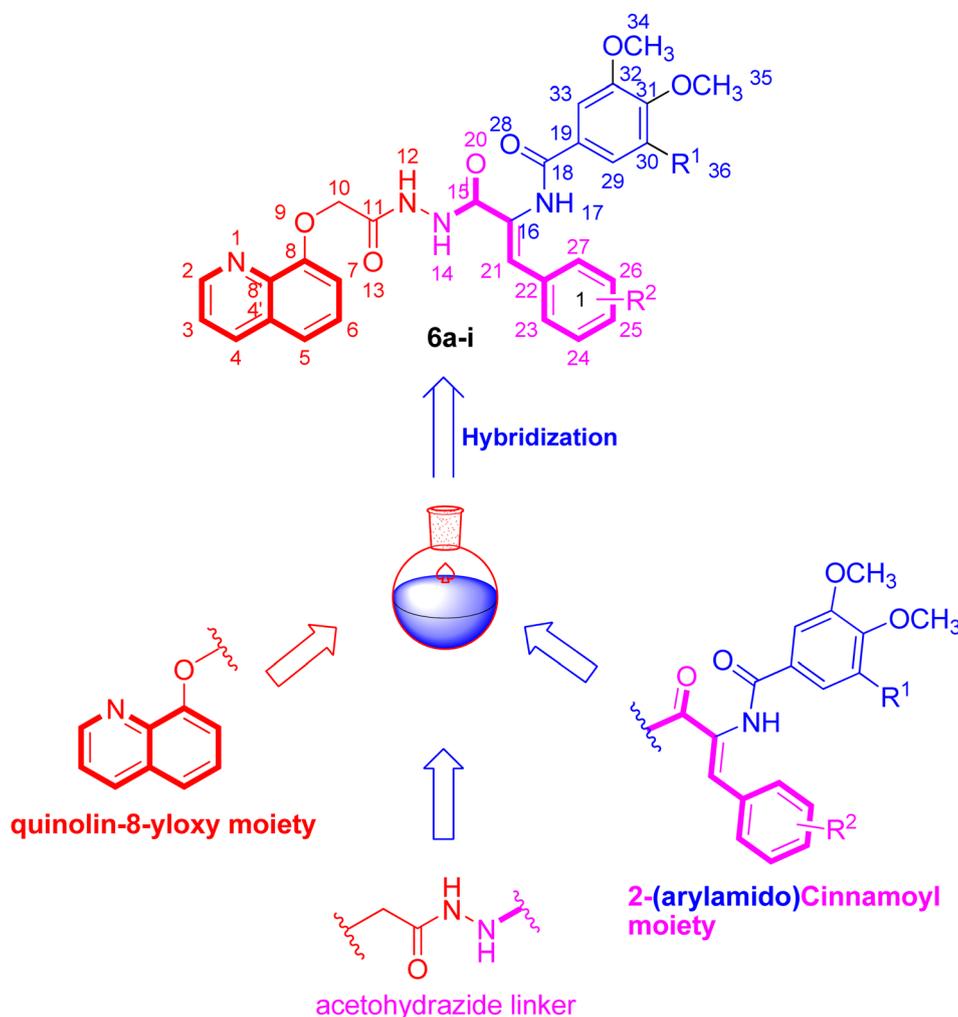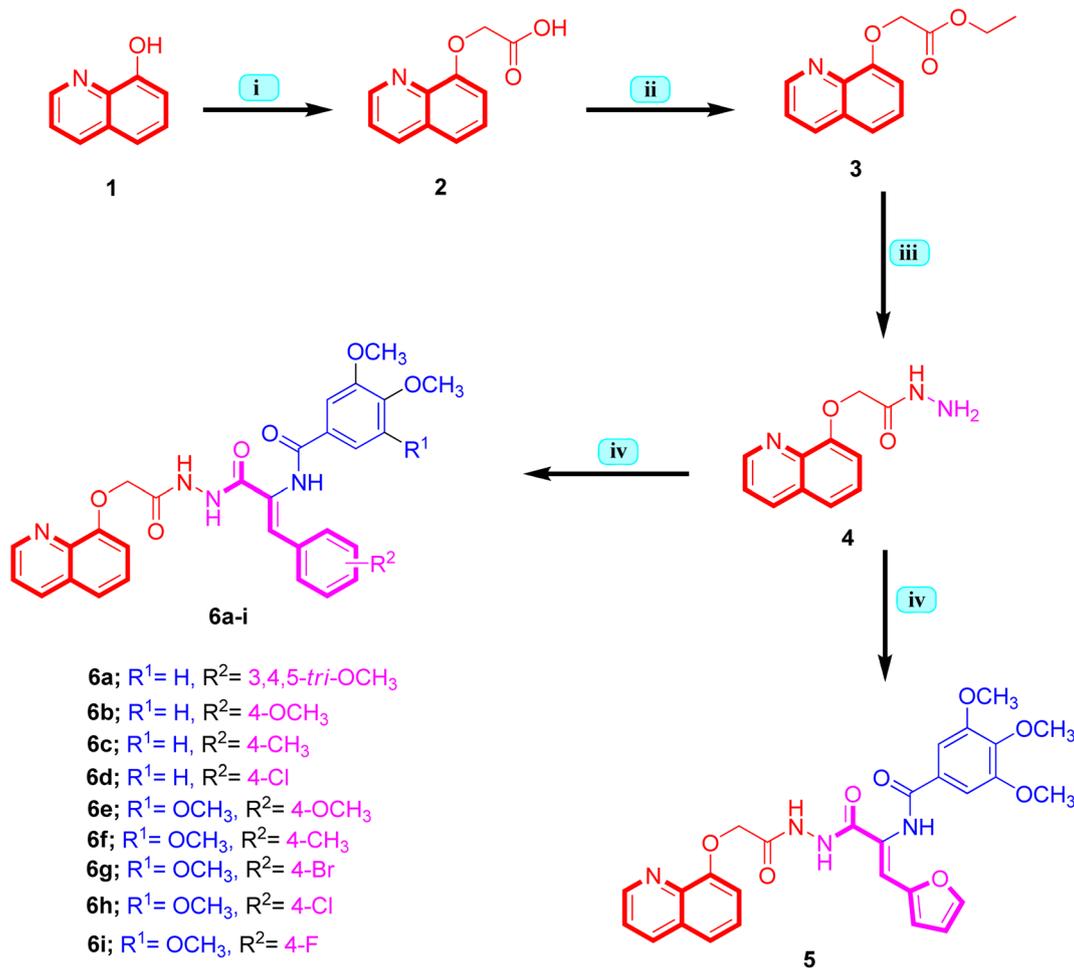

Fig. 1 Structure of the newly designed hybrids 5 and 6a–i.

© 2024 The Author(s). Published by the Royal Society of Chemistry

Scheme 1 The proposed synthetic pathway used to synthesize quinoline-cinnamide hybrids **5** and **6a–i**. Reagents: (i) ClCH$_2$COOH, anhydrous K$_2$CO$_3$, DMF, reflux 24 h; (ii) absolute ethanol, AcOH, Conc. H$_2$SO$_4$, reflux 8 h; (iii) NH$_2$NH$_2$·H$_2$O, methanol, stirring overnight; (iv) appropriate ethyl 2-(arylamido)-cinnamate derivative, EtOH, AcOH, reflux 18–20 h.

concentrated sulfuric acid to get ethyl 2-(quinoline-8-yloxy) acetate **3**. Hydrazinolysis of ethyl 2-(quinoline-8-yloxy)acetate **3** with hydrazine hydrate in methanol as solvent, 2-(quinoline-8-yloxy)acetohydrazide **4** was obtained in good yield.[33] The key 2-(quinoline-8-yloxy)acetohydrazide intermediate **4** was condensed with appropriate ethyl 2-(arylamido)-cinnamate derivatives to yield the titled quinoline-cinnamide hybrids **5** and **6a–i**. During the reaction, thin layer chromatography (TLC) was used in order to optimize the reactions, purity and completeness. The structural assignments to new hybrids were based on the elemental analysis and spectral (¹H-NMR and ¹³C-NMR) methods. ¹H-NMR spectrum of quinoline-4-methoxycinnamide hybrid **6b**, as representative example, exhibited signals (δ: 10.93, 10.16 and 9.79 ppm) ascribed to the three amide functions appeared as three singlets. In addition, the ¹H-NMR spectrum of compound **6b** was also characterized by two signals (δ: 8.89 and 8.36 ppm) appeared as doublet and doublet of doublet signals with coupling constant of 11.9, 3.3 and 8.2 Hz, respectively assigned to C2–H and C4–H of quinoline moiety, while the other aromatic protons were observed between δ 7.69–6.96 ppm. Besides, the presence of singlet signal

(δ: 7.24 ppm) ascribed to olefinic proton of cinnamide moiety. Moreover, the three methoxy groups contained in 3,4-dimethoxybenzamide and 4-methoxycinnamide moieties of the representative quinoline-4-methoxycinnamide hybrid **6b** were observed as three singlet signals (δ: 3.84, 3.83 and 3.76 ppm) integrating three protons each. Furthermore, the signal observed at δ 4.89 ppm pointing to the presence of methylene group in the hybrid compound **6b**. The ¹³C-NMR spectrum of quinoline-4-methoxycinnamide hybrid **6b** revealed four upfield signals at δ 68.18, 56.14, 56.07 and 55.68 ppm attributed to one methylene carbon and three methoxy carbons, respectively. Even though the three amide linkers' carbonyl carbons appeared downfield at δ 167.21, 165.90 and 165.03 ppm. The other peaks of carbons were observed at aromatic region in the range δ 160.20–111.35 ppm verifying that the hybrid compound **6b** possesses twenty three carbons in.

2.2. Biology

2.2.1. Cytotoxic activity against HepG2 liver cancerous cell line. To study the cytotoxic activity of the newly synthesized 2-

Table 1 The cytotoxic activity of 2-(arylamido)cinnamide tethered quinoline hybrids **5**, **6a–i** and Col against HepG2 liver cancer cell line
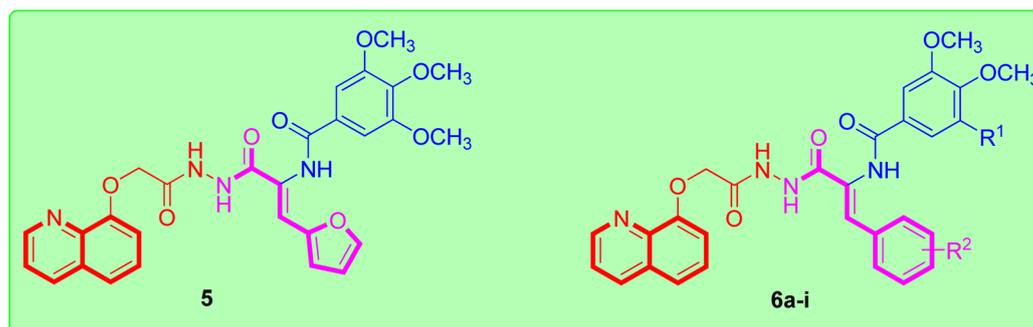
Comp no.	R^1	R^2	IC$_{50}$ value (μM) HepG2
5	—	—	4.82 ± 0.24
6a	H	3,4,5-*tri*-OCH$_3$	6.24 ± 0.36
6b	H	4-OCH$_3$	15.71 ± 0.61
6c	H	4-CH$_3$	23.48 ± 0.78
6d	H	4-Cl	26.93 ± 0.74
6e	OCH$_3$	4-OCH$_3$	2.46 ± 0.14
6f	OCH$_3$	4-CH$_3$	5.35 ± 0.32
6g	OCH$_3$	4-Br	41.31 ± 0.87
6h	OCH$_3$	4-Cl	6.79 ± 0.39
6i	OCH$_3$	4-F	6.32 ± 0.33
Col	—	—	6.09 ± 0.17

(arylamido)cinnamide tethered quinoline hybrids **5** and **6a–i**, the antiproliferative activity was evaluated using liver (HepG2) cancerous cell line which is known to possess tubulin-microtubule dysregulation.[34] The procedure of the MTT colorimetric test was used for assessing the cytotoxic potential of the synthesized hybrids. As a positive control, Colchicine (Col) was utilized, and the results obtained have been presented in Table 1 as an IC$_{50}$ (μM) values. Investigating the obtained results

toward the tested HepG2 cell line showed that the presence of 2-(3,4,5-trimethoxybenzamido)cinnamide moiety enhances the cytotoxic action of compounds **5** and **6e–i** compared with 2-(3,4-dimethoxybenzamido)cinnamide-quinoline-containing compounds **6a–d**. Importantly, the presence of electron donating group on the *para* position of cinnamide moiety in compounds **6e** and **6f** is preferred for the observed cytotoxic activity compared to electron withdrawing group containing
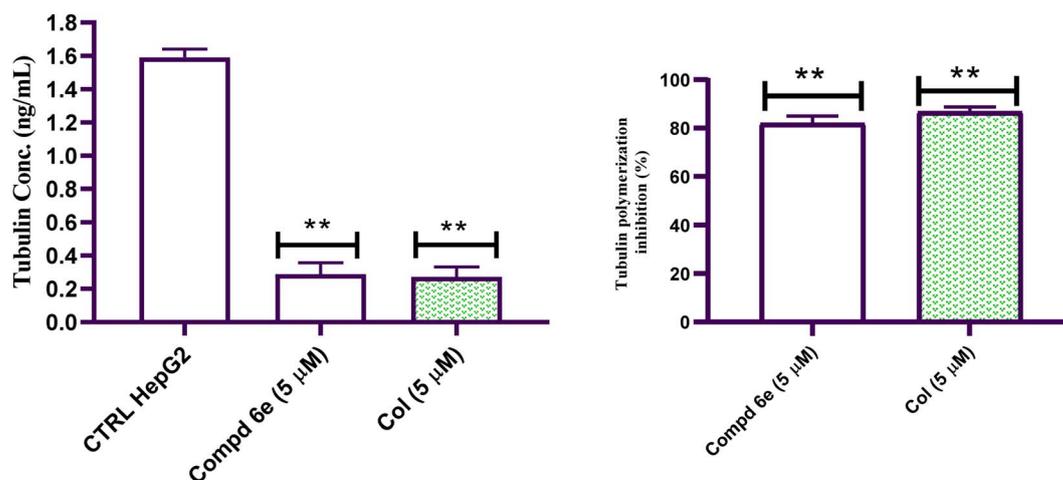

Fig. 2 Bar chart representation of tubulin inhibition of tested quinoline-4-methoxycinnamide hybrid **6e** and Col compared to untreated control HepG2 cells. All data were run as mean ± SD, and statistical analysis have been carried out using one way analysis of variance (ANOVA) test technique (*$p < 0.05$, **$p < 0.01$, ***$p < 0.001$).
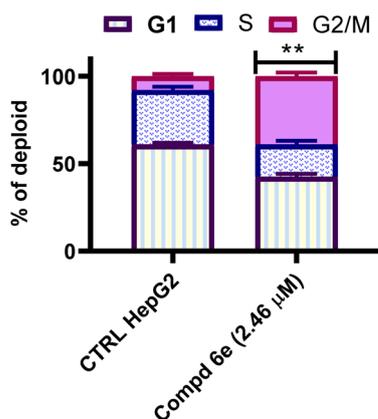
Fig. 3 Effect of quinoline-4-methoxycinnamide hybrid **6e** on the average population of cells in G1, S and G2/M phases of HepG2 cell line. All data were run as mean ± SD, and statistical analysis have been carried out using one way analysis of variance (ANOVA) test technique ($*p < 0.05$, $**p < 0.01$, $***p < 0.001$).

compounds **6b** and **6g** (Table 1). In this regard, the 2-(3,4,5-trimethoxybenzamido)cinnamide-quinolines **5** and **6e–i** possess considerable cytotoxic activity (IC$_{50}$ range: 2.46–6.79 μM), with an exception for 2-(3,4,5-trimethoxybenzamido)-4-bromocinnamide-quinoline compound **6g** (IC$_{50}$ = 41.31 μM). In particular, 2-(3,4,5-trimethoxybenzamido)-4-methoxycinnamide-quinoline hybrid **6e** was the most active against HepG2 cells with IC$_{50}$ value of 2.46 μM, which was more active than Col that demonstrated IC$_{50}$ value of 6.09 μM. In case of 2-(3,4-dimethoxybenzamido)cinnamide-quinoline hybrids **6a–d**, the antiproliferative activity 2-(3,4-dimethoxybenzamido)-3,4,5-trimethoxycinnamide-quinoline **6a** towards HepG2 cell line maintain the cytotoxic activity (IC$_{50}$ = 6.24 μM). While the remaining 2-(3,4-dimethoxybenzamido)cinnamide-quinoline molecules **6b–d** suffered a decrease in the activity with an IC$_{50}$ values ranged from 15.71 to 26.93 μM.

2.2.2. *In vitro* tubulin polymerization inhibition activity. Mechanistic research has shown that the potent cytotoxic activity of many anticancer agents is based on the inhibition of tubulin assembly.[31] To further characterize the target of selected
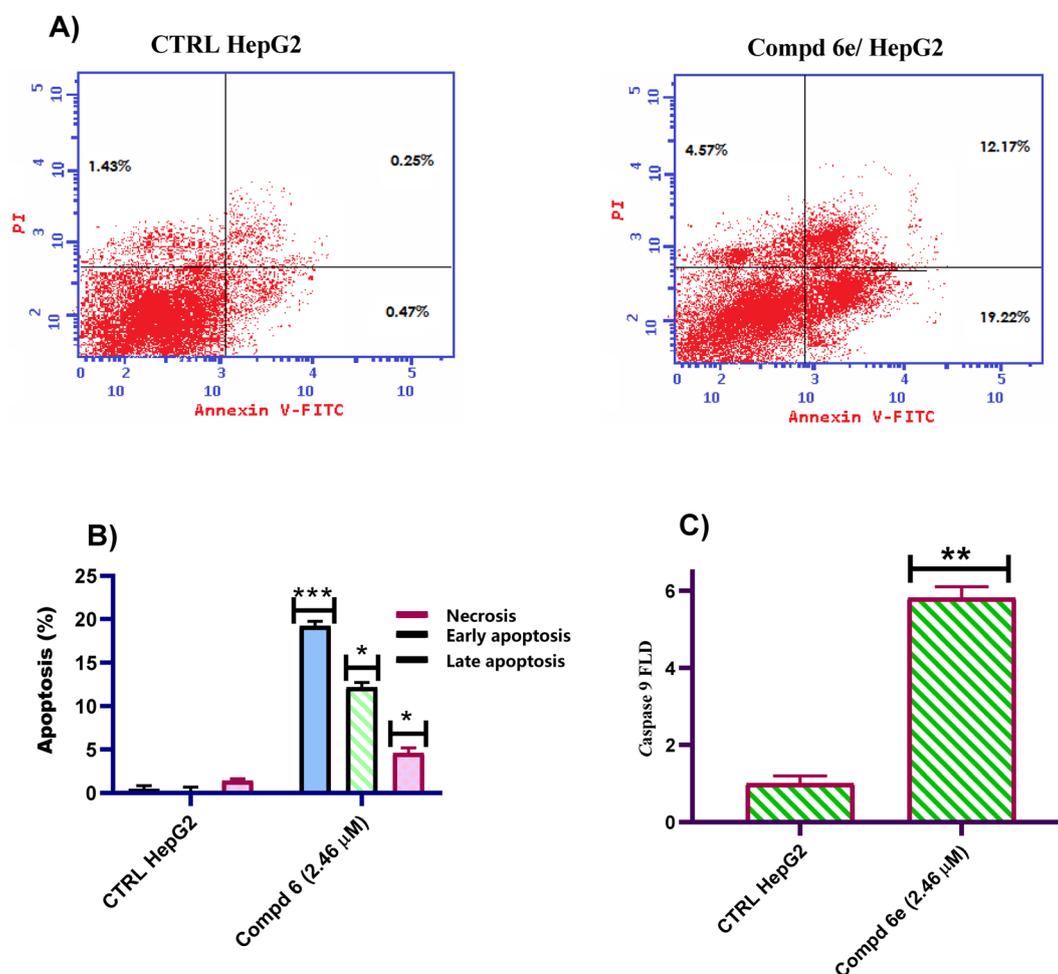
Fig. 4 (A) Effect of quinoline-4-methoxycinnamide hybrid **6e** on the proportion of Annexin V-FITC/PI in HepG2 cells; (B) bar chart representation of apoptotic induction analysis of quinoline-4-methoxycinnamide hybrid **6e** and control untreated HepG2 cells; (C) effect of quinoline-4-methoxycinnamide hybrid **6e** on active *c*aspase 9 level and compared to controls. All data were run as mean ± SD, and statistical analysis have been carried out using one way analysis of variance (ANOVA) test technique ($*p < 0.05$, $**p < 0.01$, $***p < 0.001$).

compound quinoline-4-methoxycinnamide **6e**. The *in vitro* tubulin polymerization inhibition activity of quinoline-4-methoxycinnamide hybrid **6e** was assessed as previously described.[32] Col was selected as the reference control. Compound **6e** and Col were used at 5 μM concentration and the percentage of tubulin polymerization inhibition was detected. After tubulin was incubated with quinoline-4-methoxycinnamide **6e** at the mentioned concentration, the change in absorbance was decreased compared with control untreated cells. This indicated that quinoline-4-methoxycinnamide hybrid **6e** inhibited tubulin polymerization. The percentage inhibition value of tubulin polymerization was determined as 82.01% which was slightly lower than that of Col (percent inhibition value of 86.79%). Therefore, quinoline-4-methoxycinnamide **6e** was potent inhibitor of tubulin polymerization (Fig. 2).

2.2.3. Effect of quinoline-4-methoxycinnamide 6e on HepG2 cell cycle. Microtubules play a vital role in the movement of chromosomes during cellular division.[35] As most tubulin destabilized agents disrupted the regulated cellular cycle distribution, flow cytometric analysis was performed to determine the impact of quinoline-4-methoxycinnamide hybrid **6e** on the HepG2 cell cycle. The cancerous cells were treated with the tested compounds at 2.46 μM and control for 48 h. As illustrated in Fig. 3, when HepG2 cells were exposed to quinoline-4-methoxycinnamide **6e** at the IC_{50} concentration of 2.46 μM for 48 h, 38.88% of the cells were arrested at the G2/M phase as compared with control untreated HepG2 cells (G2/M phase percentage 7.79%). Meanwhile, the proportion of cells in the G1 and S phases decreased from 61.10 and 31.11%, respectively to 42.48 and 18.64% in the quinoline-4-methoxycinnamide **6e**-treated HepG2 cells. These results indicated that quinoline-4-methoxycinnamide hybrid **6e** can block HepG2 cells at the G2/M phase in HepG2 liver cancerous cells.

2.2.4. Effect of quinoline-4-methoxycinnamide 6e on HepG2 cellular apoptosis. Mitotic arrest of cancerous cells by tubulin assembly inhibition agents is generally associated with cellular apoptosis.[36] Therefore, the apoptotic effect of quinoline-4-methoxycinnamide **6e** on HepG2 cells was assessed. As illustrated in Fig. 4A and B, after HepG2 cells were exposed to quinoline-4-methoxycinnamide hybrid **6e** at the IC_{50} concentration of 2.46 μM for 48 h, the proportion of cells that were apoptotic was determined to be 19.22 and 12.17%, respectively. These proportions were greater than that under the control untreated condition which afforded 0.47 and 0.25% apoptotic value percentage, respectively. Indicating that quinoline-4-methoxycinnamide **6e** induced HepG2 cellular apoptosis.

On the other hand, caspase is an important apoptotic protein. Therefore, the impact of quinoline-4-methoxycinnamide **6e** on the expression of initiator caspase 9 was measured using qR-PCR method. As can be seen in Fig. 4C, treating HepG2 cells with quinoline-4-methoxycinnamide **6e** at the IC_{50} concentration (2.46 μM) for 48 h, the active caspase 9 level was upregulated. The results demonstrated that quinoline-4-methoxycinnamide **6e** boosted the active caspase 9 quantity by 5.81-fold when compared to untreated control leading to cellular apoptosis.

3. Conclusions

This study represents the synthesis of a congeneric series of quinoline scaffold tethered cinnamide hybrids **5** and **6a–i** for the development of novel anticancer agents. All the synthesized hybrids were assessed for their potential cytotoxic action toward the liver (HepG2) cancerous cell line. The tested 2-(arylamido)cinnamide-quinoline derivatives **5** and **6a–i** showed moderate to outstanding cytotoxic activity with IC_{50} values ranging from 2.46–41.31 μM against HepG2 cell line. In particular, 2-(3,4,5-trimethoxybenzamido)-4-methoxycinnamide-quinoline hybrid **6e** had the highest IC_{50} value of 2.46 μM against the HepG2 cell line and outperforming to the reference drug Col (IC_{50} = 6.09 μM). The findings of tubulin polymerization inhibition assay for 2-(3,4,5-trimethoxybenzamido)-4-methoxycinnamide-quinoline hybrid **6e** showed that the tested hybrid inhibited tubulin polymerization with percentage inhibition value of 82.01% which was slightly lower than that of Col (86.79% percent inhibition value). In addition, cell cycle analysis for the most active hybrid **6e** revealed a significant drop in the cell distribution at G1 and S phases which was accompanied by marked elevation in the percentage of G/M phase, implying that the cell cycle was primarily halted at the G2/M phase in HepG2 cells. Moreover, an Annexin V-FITC/PI analytical method demonstrated that the tested 2-(3,4,5-trimethoxybenzamido)-4-methoxycinnamide-quinoline hybrid **6e** was able to induce 43.60-fold increase in HepG2 cells when compared to untreated control. Furthermore, the 2-(3,4,5-trimethoxybenzamido)-4-methoxycinnamide-quinoline hybrid **6e** boosted active caspase 9 level by 5.81-fold compared to control cells. The findings suggested that the antiproliferative activity was caused by suppression of tubulin polymerization and subsequent apoptosis induction. Collectively, these results suggested that 2-(3,4,5-trimethoxybenzamido)-4-methoxycinnamide-quinoline hybrid **6e** is a potential lead candidate for future optimization and development as promising liver cancer antitumor agent with tubulin polymerization suppression activity.

4. Experimental

4.1. General

4.1.1. Chemistry

4.1.1.1. General procedure for the synthesis of (Z)-aryl-N-(1-aryl-3-oxo-3-(2-(2-(quinolin-8-yloxy)acetyl)hydrazinyl)prop-1-en-2-yl)benzamides 5 and 6a–i. 2-(Quinoline-8-yloxy)acetohydrazide **4** (0.217 g, 1 mmol) and appropriate ethyl 2-(arylamido)cinnamate derivative (1 mmol) were dissolved in pure ethanol (20 mL) and then glacial acetic acid (10 drops) was added. After refluxing to 18–20 h, the reaction mixture was cooled down to ambient temperature and allowed to precipitate for the entire night. The crude material thus obtained was chromatographed using $(CH_2Cl_2/MeOH\ 97:3)$ to get the required quinoline-cinnamide hybrids.

(Z)-N-(1-(Furan-2-yl)-3-oxo-3-(2-(2-(quinolin-8-yloxy)acetyl)hydrazinyl)prop-1-en-2-yl)-3,4,5-trimethoxybenzamide (5): Yield: 62%, m.p. 249–251 °C. Analysis: calc. for $C_{28}H_{26}N_4O_8$ (546.53): C 61.53, H 4.80, N 10.25%, found: C 61.59, H 4.84, N 10.18%. ^{1}H-

NMR (400 MHz, DMSO-d_6) δ: 10.43 (d, J = 9.9 Hz, 1H, NH), 10.23 (s, 1H, NH), 9.70 (d, J = 111.6 Hz, 1H, NH), 8.90 (d, J = 3.5 Hz, 1H, C2–H quinoline), 8.36 (d, J = 8.2 Hz, 1H, C4–H quinoline), 7.83 (d, J = 20.4 Hz, 1H, Ar–H), 7.64–7.56 (m, 2H, Ar–H), 7.56–7.50 (m, 1H, Ar–H), 7.39 (s, 2H, Ar–H), 7.29 (d, J = 7.6 Hz, 1H, Ar–H), 7.19 (s, 1H, olefinic CH), 6.77 (d, J = 3.2 Hz, 1H, furan CH), 6.61 (s, 1H, furan CH), 4.89 (s, 2H, OCH_2), 3.87 (s, 6H, 2OCH_3), 3.75 (s, 3H, OCH_3). ^{13}C-NMR (DMSO, 101 MHz) δ: 166.80, 165.20, 163.68, 153.88, 152.54, 149.49, 149.30, 144.86, 140.34, 139.78, 136.01, 129.11, 128.92, 126.71, 125.80, 121.99, 120.95, 118.21, 114.53, 112.39, 111.64, 105.59, 67.70 (OCH_2), 60.12 (OCH_3), 56.07 (2OCH_3) ppm.

(Z)-3,4-Dimethoxy-N-(3-oxo-3-(2-(2-(quinolin-8-yloxy)acetyl) hydraziny1)-1-(3,4,5-trimethoxyphenyl)prop-1-en-2-yl)benzamide (6a): Yield: 65%, m.p. 233–235 °C. Analysis: calc. for $C_{32}H_{32}N_4O_9$ (616.62): C 62.33, H 5.23, N 9.09%, found: C 62.22, H 5.31, N 8.96%. ^{1}H-NMR (400 MHz, DMSO-d_6) δ: 10.44 (d, J = 12.1 Hz, 1H, NH), 10.24 (s, 1H, NH), 9.85 (s, 1H, NH), 8.91 (d, J = 2.9 Hz, 1H, C2–H quinoline), 8.36 (d, J = 7.6 Hz, 1H, C4–H quinoline), 7.70 (d, J = 8.6 Hz, 1H, Ar–H), 7.67 (s, 1H, Ar–H), 7.62–7.56 (m, 2H, Ar–H), 7.53 (t, J = 7.9 Hz, 1H, Ar–H), 7.31 (d, J = 4.4 Hz, 2H, Ar–H and olefinic CH), 7.09–7.04 (m, 1H, Ar–H), 6.99 (s, 2H, Ar–H), 4.90 (s, 2H, OCH_2), 3.84 (s, 3H, OCH_3), 3.81 (s, 3H, OCH_3), 3.66 (s, 3H, OCH_3), 3.62 (s, 6H, 2OCH_3). ^{13}C-NMR (DMSO, 101 MHz) δ: 167.19, 165.89, 164.75, 154.37, 153.03, 152.16, 149.77, 148.58, 140.26, 138.57, 136.47, 130.97, 129.77, 129.57, 128.40, 127.18, 126.27, 122.46, 121.93, 121.40, 112.11, 111.67, 111.24, 107.64, 68.18 (OCH_2), 60.52 (OCH_3), 56.12 (OCH_3), 56.10 (OCH_3), 56.07 (2OCH_3).

(Z)-3,4-Dimethoxy-N-(1-(4-methoxypheny1)-3-oxo-3-(2-(2-(quinolin-8-yloxy)acetyl) hydrazinyl)prop-1-en-2-yl)benzamide (6b): Yield: 69%, m.p. 281–283 °C. Analysis: calc. for $C_{30}H_{28}N_4O_7$ (556.57): C 64.74, H 5.07, N 10.07%, found: C 64.61, H 4.90, 10.19.68%. ^{1}H-NMR (400 MHz, DMSO-d_6) δ: 10.39 (s, 1H, NH), 10.16 (s, 1H, NH), 9.79 (s, 1H, NH), 8.89 (dd, J = 11.9, 3.3 Hz, 1H, C2–H quinoline), 8.36 (d, J = 8.3 Hz, 1H, C4–H quinoline), 7.69 (t, J = 8.5 Hz, 1H, Ar–H), 7.62 (s, 2H, Ar–H), 7.58 (d, J = 3.9 Hz, 2H, Ar–H), 7.57–7.50 (m, 2H, Ar–H), 7.30 (d, J = 7.5 Hz, 1H, Ar–H), 7.24 (s, 1H, olefinic CH), 7.08 (d, J = 8.4 Hz, 1H, Ar–H), 6.96 (dd, J = 15.9, 8.7 Hz, 2H, Ar–H), 4.89 (s, 2H, OCH_2), 3.84 (s, 3H, OCH_3), 3.83 (s, 3H, OCH_3), 3.76 (s, 3H, OCH_3). ^{13}C-NMR (DMSO, 101 MHz) δ: 167.21, 165.90, 165.03, 160.20, 154.36, 152.11, 149.77, 148.63, 140.26, 136.46, 131.72, 130.40, 129.57, 127.18, 127.07, 126.92, 126.44, 122.45, 121.86, 121.39, 114.53, 112.10, 111.80, 111.35, 68.18 (OCH_2), 56.14 (OCH_3), 56.07 (OCH_3), 55.68 (OCH_3).

(Z)-3,4-Dimethoxy-N-(3-oxo-3-(2-(2-(quinolin-8-yloxy) acetyphydraziny1)-1-p-tolylprop-1-en-2-yl)benzamide (6c): Yield: 71%, m.p. 275–277 °C. Analysis: calc. for $C_{30}H_{28}N_4O_6$ (540.57): C 66.66, H 5.22, N 10.36%, found: C 66.82, H 5.13, N 10.24%. ^{1}H NMR (400 MHz, DMSO-d_6) δ: 10.44 (d, J = 14.3 Hz, 1H, NH), 10.16 (d, J = 59.9 Hz, 1H, NH), 9.83 (s, 1H, NH), 9.03–8.83 (m, 1H, C2–H quinoline), 8.36 (d, J = 8.0 Hz, 1H, C4–H quinoline), 7.70–7.64 (m, 1H, Ar–H), 7.60 (d, J = 9.2 Hz, 2H, Ar–H), 7.56 (dd, J = 12.8, 6.1 Hz, 2H, Ar–H), 7.50 (d, J = 8.2 Hz, 2H, Ar–H), 7.30 (d, J = 7.5 Hz, 1H, Ar–H), 7.23 (s, 1H, olefinic CH), 7.18 (d, J =

7.8 Hz, 2H, Ar–H), 7.14–7.05 (m, 1H, Ar–H), 4.90 (s, 2H, OCH_2), 3.85 (s, 3H, OCH_3), 3.83 (s, 3H, OCH_3), 2.29 (s, 3H, CH_3). ^{13}C-NMR (DMSO, 101 MHz) δ: 167.24, 165.92, 164.96, 154.37, 152.14, 149.77, 148.64, 140.26, 139.07, 136.47, 131.68, 130.29, 129.97, 129.62, 129.57, 128.55, 127.19, 126.40, 122.46, 121.87, 121.41, 112.12, 111.79, 111.35, 68.19 (OCH_2), 56.14 (OCH_3), 56.07 (OCH_3), 21.37 (CH_3).

(Z)-N-(1-(4-Chloropheny1)-3-oxo-3-(2-(2-(quinolin-8-yloxy) acetyl)hydrazinyl)prop-1-en-2-y1)-3,4-dimethoxybenzamide (6d): Yield: 74%, m.p. 250–252 °C. Analysis: calc. for $C_{29}H_{25}ClN_4O_6$ (560.98): C 62.09, H 4.49, N 9.99%, found: C 61.94, H 4.57, N 10.11%. ^{1}H-NMR (400 MHz, DMSO-d_6) δ: 10.44 (s, 1H, NH), 10.30 (s, 1H, NH), 9.88 (s, 1H, NH), 8.91 (dd, J = 4.1, 1.6 Hz, 1H, C2–H quinoline), 8.36 (dd, J = 8.3, 1.6 Hz, 1H, C4–H quinoline), 7.65 (t, J = 7.5 Hz, 1H, Ar–H), 7.61 (s, 1H, Ar–H), 7.58 (d, J = 4.6 Hz, 3H, Ar–H), 7.57–7.52 (m, 1H, Ar–H), 7.52–7.47 (m, 1H, Ar–H), 7.44 (d, J = 8.6 Hz, 2H, Ar–H), 7.29 (d, J = 6.8 Hz, 1H, Ar–H), 7.19 (s, 1H, olefinic CH), 7.08 (d, J = 8.6 Hz, 1H, Ar–H), 4.89 (s, 2H, OCH_2), 3.84 (s, 3H, OCH_3), 3.82 (s, 3H, OCH_3). ^{13}C-NMR (DMSO, 101 MHz) δ: 167.23, 165.89, 164.75, 154.38, 152.23, 149.78, 148.66, 140.28, 136.46, 133.63, 133.51, 131.53, 130.12, 129.57, 129.06, 128.38, 127.18, 126.18, 122.45, 121.94, 121.42, 112.15, 111.78, 111.36, 68.20 (OCH_2), 56.49 (OCH_3), 56.08 (OCH_3).

(Z)-3,4,5-Trimethoxy-N-(1-(4-methoxyphenyl)-3-oxo-3-(2-(2-(quinolin-8-yloxy)acetylhydrazinyl)prop-1-en-2-yl)benzamide (6e): Yield: 63%, m.p. 258–260 °C. Analysis: calc. for $C_{31}H_{30}N_4O_8$ (586.59): C 63.47, H 5.15, N 9.55%, found: C 63.36, H 5.02, N 9.66%. ^{1}H-NMR (400 MHz, DMSO-d_6) δ 10.40 (d, J = 10.5 Hz, 1H, NH), 10.16 (d, J = 15.6 Hz, 1H, NH), 9.89 (s, 1H, NH), 8.89 (dd, J = 13.2, 2.8 Hz, 1H, C2–H quinoline), 8.36 (d, J = 7.3 Hz, 1H, C4–H quinoline), 7.66–7.61 (m, 1H, Ar–H), 7.59 (s, 2H, Ar–H), 7.57 (s, 1H, Ar–H), 7.56–7.50 (m, 1H, Ar–H), 7.38 (s, 2H, Ar–H), 7.30 (d, J = 7.4 Hz, 1H, Ar–H), 7.26 (s, 1H, olefinic CH), 6.98 (dd, J = 14.9, 8.8 Hz, 2H, Ar–H), 4.89 (s, 2H, OCH_2), 3.86 (s, 6H, 2OCH_3), 3.76 (s, 3H, OCH_3), 3.74 (s, 3H, OCH_3). ^{13}C-NMR (DMSO, 101 MHz) δ: 169.01, 167.26, 165.78, 164.94, 160.27, 154.37, 153.00, 149.77, 140.81, 140.26, 136.46, 131.77, 130.52, 129.57, 129.26, 127.18, 126.82, 122.45, 121.40, 114.58, 112.09, 106.07, 68.17 (OCH_2), 60.58 (OCH_3), 56.53 (2OCH_3), 55.70 (OCH_3).

(Z)-3,4,5-Trimethoxy-N-(3-oxo-3-(2-(2-(quinolin-8-yloxy) acetylhydrazinyl)-1-p-tolylprop-1-en-2-yl)benzamide (6f): Yield: 72%, m.p. 264–266 °C. Analysis: calc. for $C_{31}H_{30}N_4O_7$ (570.59): C 65.25, H 5.30, N 9.82%, found: C 65.37, H 5.43, N 9.71%. ^{1}H-NMR (400 MHz, DMSO-d_6) δ 10.45 (d, J = 23.0 Hz, 1H, NH), 10.22 (d, J = 27.5 Hz, 1H, NH), 9.93 (s, 1H, NH), 8.96–8.85 (m, 1H, C2–H quinoline), 8.41–8.29 (m, 1H, C4–H quinoline), 7.63–7.56 (m, 2H, Ar–H), 7.55 (s, 1H, Ar–H), 7.53 (d, J = 4.1 Hz, 1H, Ar–H), 7.51 (d, J = 4.0 Hz, 1H, Ar–H), 7.38 (s, 2H, Ar–H), 7.30 (d, J = 7.5 Hz, 1H, Ar–H), 7.25 (s, 1H, olefinic CH), 7.20 (d, J = 7.9 Hz, 2H, Ar–H), 4.90 (s, 2H, OCH_2), 3.86 (s, 6H, 2OCH_3), 3.75 (s, 3H, OCH_3), 2.29 (s, 3H, CH_3). ^{13}C-NMR (DMSO, 101 MHz) δ: 167.28, 165.80, 164.86, 154.36, 153.01, 149.77, 140.85, 140.25, 139.17, 136.47, 131.58, 130.43, 130.00, 129.67, 129.57, 129.21, 128.36, 127.18, 122.45, 121.41, 112.10, 106.07, 68.18 (OCH_2), 60.58 (OCH_3), 56.53 (2OCH_3), 21.37 (CH_3).

(Z)-N-(1-(4-Bromophenyl)-3-oxo-3-(2-(2-(quinolin-8-yloxy) acetyl)hydrazinyl)prop-1-en-2-yl)-3,4,5-trimethoxybenzamide (6g): Yield: 76%, m.p. 279–281 °C. Analysis: calc. for $C_{30}H_{27}BrN_4O_7$ (635.46): C 56.70, H 4.28, N 8.82%, found: C 56.84, H 4.22, N 8.93%. ^{1}H-NMR (400 MHz, DMSO-d_6) δ 10.50 (d, $J = 38.7$ Hz, 1H, NH), 10.28 (d, $J = 40.5$ Hz, 1H, NH), 9.98 (s, 1H, NH), 8.96–8.84 (m, 1H, C2–H quinoline), 8.42–8.29 (m, 1H, C4–H quinoline), 7.62 (d, $J = 7.7$ Hz, 2H, Ar–H), 7.59 (s, 2H, Ar–H), 7.58–7.54 (m, 2H, Ar–H), 7.52 (d, $J = 8.4$ Hz, 1H, Ar–H), 7.35 (s, 2H, Ar–H), 7.30 (d, $J = 7.5$ Hz, 1H, Ar–H), 7.20 (s, 1H, olefinic CH), 4.90 (s, 2H, OCH_2), 3.86 (s, 6H, 2OCH_3), 3.74 (s, 3H, OCH_3). ^{13}C-NMR (DMSO, 101 MHz) δ: 167.28, 165.77, 164.66, 154.36, 153.02, 149.77, 140.94, 140.26, 136.47, 133.75, 132.13, 132.05, 131.80, 130.00, 129.57, 128.99, 128.63, 127.18, 122.49, 121.43, 112.13, 106.09, 68.19 (OCH$_2$), 60.58 (OCH$_3$), 56.50 (2OCH$_3$).

(Z)-N-(1-(4-Chlorophenyl)-3-oxo-3-(2-(2-(quinolin-8-yloxy)acety) hydrazinyl)prop-1-en-2-yl)-3,4,5-trimethoxybenzamide (6h): Yield: 71%, m.p. 243–245 °C. Analysis: calc. for $C_{30}H_{27}ClN_4O_7$ (591.01): C 60.97, H 4.60, N 9.48%, found: C 61.08, H 4.47, N 9.43%. ^{1}H-NMR (400 MHz, DMSO-d_6) δ: 10.52 (d, $J = 36.4$ Hz, 1H, NH), 10.30 (d, $J = 38.4$ Hz, 1H, NH), 9.99 (s, 1H, NH), 8.97–8.84 (m, 1H, C2–H quinoline), 8.42–8.30 (m, 1H, C4–H quinoline), 7.70–7.63 (m, 1H, Ar–H), 7.61 (s, 1H, Ar–H), 7.59 (s, 1H, Ar–H), 7.58–7.54 (m, 1H, Ar–H), 7.54–7.50 (m, 1H, Ar–H), 7.46 (d, $J = 8.5$ Hz, 2H, Ar–H), 7.36 (s, 2H, Ar–H), 7.30 (d, $J = 7.5$ Hz, 1H, Ar–H), 7.23 (s, 1H, olefinic CH), 4.91 (s, 2H, OCH_2), 3.86 (s, 6H, 2OCH_3), 3.74 (s, 3H, OCH_3). ^{13}C-NMR (DMSO, 101 MHz) δ: 171.72, 167.30, 165.80, 164.66, 154.36, 153.03, 149.76, 140.94, 140.25, 136.48, 133.75, 133.40, 131.57, 129.91, 129.57, 129.12, 129.00, 128.62, 127.17, 122.45, 121.43, 112.13, 106.09, 68.20 (OCH$_2$), 60.57 (OCH$_3$), 56.54 (2OCH$_3$).

(Z)-N-(1-(4-Fluorophenyl)-3-oxo-3-(2-(2-(quinolin-8-yloxy)acety) hydrazinyl)prop-1-en-2-yl)-3,4,5-trimethoxybenzamide (6i): Yield: 68%, m.p. 236–238 °C. Analysis: calc. for $C_{30}H_{27}FN_4O_7$ (574.56): C 62.71, H 4.74, N 9.75%, found: C 62.64, H 4.68, N 9.90%. ^{1}H-NMR (400 MHz, DMSO-d_6) δ 10.46 (d, $J = 32.5$ Hz, 1H, NH), 10.24 (d, $J = 28.5$ Hz, 1H, NH), 9.95 (s, 1H, NH), 8.90 (dd, $J = 4.1$, 1.6 Hz, 1H, C2–H quinoline), 8.37 (dd, $J = 8.3$, 1.6 Hz, 1H, C4–H quinoline), 7.72 (dd, $J = 8.5$, 5.8 Hz, 1H, Ar–H), 7.66 (dd, $J = 8.5$, 5.6 Hz, 2H, Ar–H), 7.59 (dt, $J = 8.9$, 4.7 Hz, 2H, Ar–H), 7.56–7.50 (m, 1H, Ar–H), 7.36 (s, 2H, Ar–H), 7.33–7.26 (m, 2H, Ar–H), 7.25 (s, 1H, olefinic CH), 4.89 (s, 2H, OCH_2), 3.85 (s, 6H, 2OCH_3), 3.74 (s, 3H, OCH_3). ^{13}C-NMR (DMSO, 101 MHz) δ: 167.27, 165.83, 164.72, 154.38, 153.02, 149.77, 140.90, 140.28, 136.46, 132.19, 132.11, 131.00, 129.57, 129.06, 129.01, 127.17, 122.45, 121.42, 116.19, 115.98, 112.12, 106.08, 68.19 (OCH$_2$), 60.58 (OCH$_3$), 56.49 (2OCH$_3$).

4.2. Biological studies

All experimental procedures used in the biological evaluations were shown in the ESI.†

Conflicts of interest

The authors report no conflicts of interest.

Acknowledgements

References

1 Z. Yu, X. Bai, R. Zhou, G. Ruan, M. Guo, W. Han, S. Jiang and H. Yang, Differences in the incidence and mortality of digestive cancer between Global Cancer Observatory 2020 and Global Burden of Disease 2019, *Int. J. Cancer*, 2024, **154**, 615–625.

2 R. L. Siegel, A. N. Giaquinto and A. Jemal, *Cancer statistics, 2024.* CA: A Cancer, *J. Clin.*, 2024, **74**, 12–49.

3 Brianna and S. H. Lee, Chemotherapy: how to reduce its adverse effects while maintaining the potency?, *Med. Oncol.*, 2023, **40**, 88–99.

4 H. Tian, T. Zhang, S. Qin, Z. Huang, L. Zhou, J. Shi, E. C. Nice, N. Xie, C. Huang and Z. Shen, Enhancing the therapeutic efficacy of nanoparticles for cancer treatment using versatile targeted strategies, *J. Hematol. Oncol.*, 2022, **15**, 132–149.

5 Q.-Q. Zhou, H.-T. Xiao, F. Yang, Y.-D. Wang, P. Li and Z.-G. Zheng, Advancing targeted protein degradation for metabolic diseases therapy, *Pharmacol. Res.*, 2023, **188**, 106627–106642.

6 X. Wang, B. Gigant, X. Zheng and Q. Chen, Microtubule-targeting agents for cancer treatment: Seven binding sites and three strategies, *MedComm: Oncol.*, 2023, **2**, e46.

7 A. Falconieri, A. Coppini and V. Raffa, Microtubules as a signal hub for axon growth in response to mechanical force, *Biol. Chem.*, 2024, **405**, 67–77.

8 E. D. McKenna, S. L. Sarbanes, S. W. Cummings and A. Roll-Mecak, The Tubulin Code, from Molecules to Health and Disease, *Annu. Rev. Cell Dev. Biol.*, 2023, **39**, 331–361.

9 I. Zaki, M. K. Abdelhameid, I. M. El-Deen, A. H. A. Abdel Wahab, A. M. Ashmawy and K. O. Mohamed, Design, synthesis and screening of 1, 2, 4-triazinone derivatives as potential antitumor agents with apoptosis inducing activity on MCF-7 breast cancer cell line, *Eur. J. Med. Chem.*, 2018, **156**, 563–579.

10 H. M. Abd El-Lateef, L. M. A. Ghany, R. M. Saleem, A. H. A. Maghrabi, M. A. Y. Alahdal, E. H. K. Ali, B. Y. Beshay, I. Zaki and R. E. Masoud, Design, synthesis and antiproliferative screening of newly synthesized coumarin-acrylamide hybrids as potential cytotoxic and apoptosis inducing agents, *RSC Adv.*, 2023, **13**, 32547–32557.

11 M. Podolak, S. Holota, Y. Deyak, K. Dziduch, R. Dudchak, M. Wujec, K. Bielawski, R. Lesyk and A. Bielawska, Tubulin inhibitors. Selected scaffolds and main trends in the design of novel anticancer and antiparasitic agents, *Bioorg. Chem.*, 2024, **143**, 107076–107088.

12 M. N. Peerzada, M. S. Dar and S. Verma, Development of tubulin polymerization inhibitors as anticancer agents, *Expert Opin. Ther. Pat.*, 2023, **33**, 797–820.

13 O. F. Elebiju, O. O. Ajani, G. O. Oduselu, T. A. Ogunnupebi and E. Adebiyi, Recent advances in functionalized quinoline scaffolds and hybrids—Exceptional pharmacophore in therapeutic medicine, *Front. Chem.*, 2023, **10**, 1074331–1074342.

14 P. Yadav and K. Shah, Quinolines, a perpetual, multipurpose scaffold in medicinal chemistry, *Bioorg. Chem.*, 2021, **109**, 104639–104653.

15 O. O. Ajani, K. T. Iyaye and O. T. Ademosun, Recent advances in chemistry and therapeutic potential of functionalized quinoline motifs–a review, *RSC Adv.*, 2022, **12**, 18594–18614.

16 S. Tyagi, A. Mazumder, R. Kumar, V. Datt, K. Shabana, M. S. Yar and M. J. Ahsan, Synthesis and SAR of Potential Anti-Cancer Agents of Quinoline Analogues: A Review, *Med. Chem.*, 2023, **19**, 785–812.

17 N. Chirra, G. Udigala, E. O. Sinegubova, D. Nagineni, R. K. Bollikanda, Y. L. Esaulkova, A. A. Muryleva, V. V. Zarubaev and S. Kantevari, Synthesis and antiviral activity of 2-substituted 4-aminoquinoline and its analogous derivatives, *J. Heterocycl. Chem.*, 2023, **60**, 1416–1426.

18 C.-X. Liu, X. Zhao, L. Wang and Z.-C. Yang, Quinoline derivatives as potential anti-tubercular agents: Synthesis, molecular docking and mechanism of action, *Microb. Pathog.*, 2022, **165**, 105507–105519.

19 S. Sharma, K. Singh and S. Singh, Synthetic Strategies for Quinoline Based Derivatives as Potential Bioactive Heterocycles, *Curr. Org. Synth.*, 2023, **20**, 606–629.

20 X. Wang, Y. Zhuang, Y. Wang, M. Jiang and L. Yao, The recent developments of camptothecin and its derivatives as potential anti-tumor agents, *Eur. J. Med. Chem.*, 2023, **260**, 115710–115722.

21 N. P. Aijijiyah, F. A. Wati, R. Rahayu, A. Srilistiani, F. Mahzumi, T. Aulia, L. Santoso, E. Pamela, E. Y. Ramadhani, Y. A. Ilfahmi, A. S. Purnomo, S. R. Putra, E. Santoso, S. Ningsih, N. Firdausi and M. Santoso, Synthesis, α-glucosidase inhibitory activity, and molecular docking of cinnamamides, *Med. Chem. Res.*, 2023, **32**, 723–735.

22 B. Zhang, Z. Xu, Q. Liu, S. Xia, Z. Liu, Z. Liao and S. Gou, Design, synthesis and biological evaluation of cinnamamide-quinazoline derivatives as potential EGFR inhibitors to reverse T790M mutation, *Bioorg. Chem.*, 2021, **117**, 105420–105437.

23 K. Donthiboina, P. Anchi, S. Gurram, G. Sai Mani, J. Lakshmi Uppu, C. Godugu, N. Shankaraiah and A. Kamal, Synthesis and biological evaluation of substituted N-(2-(1H-benzo[d]imidazole-2-yl)phenyl)cinnamides as tubulin polymerization inhibitors, *Bioorg. Chem.*, 2020, **103**, 104191–104203.

24 S. Sana, V. G. Reddy, T. Srinivasa Reddy, R. Tokala, R. Kumar, S. K. Bhargava and N. Shankaraiah, Cinnamide derived pyrimidine-benzimidazole hybrids as tubulin inhibitors: Synthesis, *in silico* and cell growth inhibition studies, *Bioorg. Chem.*, 2021, **110**, 104765–104778.

25 M. M. Alam, A. H. E. Hassan, K. W. Lee, M. C. Cho, J. S. Yang, J. Song, K. H. Min, J. Hong, D.-H. Kim and Y. S. Lee, Design, synthesis and cytotoxicity of chimeric erlotinib-alkylphospholipid hybrids, *Bioorg. Chem.*, 2019, **84**, 51–62.

26 S. M. Aboukhatwa, P. A. Sidhom, A. Angeli, C. T. Supuran and H. O. Tawfik, Terminators or Guardians? Design, Synthesis, and Cytotoxicity Profiling of Chalcone-Sulfonamide Hybrids, *ACS Omega*, 2023, **8**, 7666–7683.

27 X.-J. Fu, J. Huang, N. Li, Y.-H. Liu, Q.-G. Liu, S. Yuan, Y. Xu, Y.-F. Chen, Y.-X. Zhao, J. Song, S.-Y. Zhang and Y.-R. Bai, Design, synthesis and biological evaluation of N-benzylaryl cinnamide derivatives as tubulin polymerization inhibitors capable of promoting YAP degradation with potent anti-gastric cancer activities, *Eur. J. Med. Chem.*, 2023, **262**, 115883–115898.

28 H. Zhu, R. Zhou, D. Cao, J. Tang and M. Li, A pharmacophore-guided deep learning approach for bioactive molecular generation, *Nat. Commun.*, 2023, **14**, 6234–6241.

29 P. Das, S. Ganguly, A. Rosenkranz, B. Wang, J. Yu, S. Srinivasan and A. R. Rajabzadeh, MXene/0D nanocomposite architectures: Design, properties and emerging applications, *Mater. Today Nano*, 2023, **24**, 100428.

30 X.-Q. Wang, L.-X. Liu, Y. Li, C.-J. Sun, W. Chen, L. Li, H.-B. Zhang and X.-D. Yang, Design, synthesis and biological evaluation of novel hybrid compounds of imidazole scaffold-based 2-benzylbenzofuran as potent anticancer agents, *Eur. J. Med. Chem.*, 2013, **62**, 111–121.

31 H. M. A. El-Lateef, R. M. Saleem, M. A. Bazuhair, A. H. A. Maghrabi, E. H. K. Ali, I. Zaki and R. E. Masoud, Design, synthesis and tubulin polymerization inhibition activity of newly synthesized hydrazone-linked to combretastatin analogues as potential anticancer agents, *J. Mol. Struct.*, 2023, **1292**, 136190–136207.

32 K. O. Mohamed, I. Zaki, I. M. El-Deen and M. K. Abdelhameid, A new class of diamide scaffold: Design, synthesis and biological evaluation as potent antimitotic agents, tubulin polymerization inhibition and apoptosis inducing activity studies, *Bioorg. Chem.*, 2019, **84**, 399–409.

33 M. Cacic, M. Trkovnik, F. Cacic and E. Has-Schon, Synthesis and Antimicrobial Activity of Some Derivatives on the Basis (7-hydroxy-2-oxo-2H-chromen-4-yl)-acetic Acid Hydrazide), *Molecules*, 2006, **11**, 134–147.

34 Y. Tian, A. Yang, H. Huang, J. Xie, L. Wang, D. Liu, X. Wei, P. Tan, P. Tu, D. Fu and Z. Hu, A novel pyrrolidine-2,5-dione derivative induced G2/M phase arrest and apoptosis of hepatocellular carcinoma HepG2 cells through inhibiting tubulin polymerization, *Arabian J. Chem.*, 2024, **17**, 105550–105562.

35 J. Sebastian and K. Rathinasamy, Microtubules and Cell Division: Potential Pharmacological Targets in Cancer Therapy, *Curr. Drug Targets*, 2023, **24**, 889–918.

36 L. Huang, Y. Peng, X. Tao, X. Ding, R. Li, Y. Jiang and W. Zuo, Microtubule Organization Is Essential for Maintaining Cellular Morphology and Function, *Oxid. Med. Cell. Longevity*, 2022, **2022**, 1623181–1623194.